Appl. Magn. Reson. 16, 237–245 (1999)

Applied Magnetic Resonance

© Springer-Verlag 1999
Printed in Austria

A Multifrequency-Resonator-Based System for High-Sensitivity High-Field EPR Investigations of Small Single Crystals

S. Hill[1], N. S. Dalal[2], and J. S. Brooks[3]

[1] Department of Physics, Montana State University, Bozeman, Montana, USA
[2] Department of Chemistry and National High Magnetic Field Laboratory, Florida State University, Tallahassee, Florida, USA
[3] Department of Physics and National High Magnetic Field Laboratory, Florida State University, Tallahassee, Florida, USA

Received May 11, 1998; revised February 15, 1999

Abstract. In this paper, we describe a multifrequency spectroscopic system which is ideally suited to EPR investigations of very small single crystals. Our method utilizes oversized resonant cavities and a continuously tunable vector network analyzer. This system provides excellent sensitivity over a broad frequency range from about 30 GHz up to about 120 GHz, and in magnetic fields up to 33 T.

1 Introduction

Spectroscopists exploring the microwave and millimeter-wave spectral ranges (3–300 GHz) are faced with a variety of challenges which stem primarily from two different problems: first, sources, detectors and all other components used in this frequency range have limited bandwidths; second, the wavelengths in this spectral range (1 mm to 10 cm) rule out any possibility of performing conventional optical spectroscopy, especially within the restricted space provided inside the bore of a high-field magnet.

These disadvantages may be partially compensated for by the use of resonant techniques and narrow-band detection schemes to achieve a much higher relative sensitivity as compared to conventional single-pass spectroscopic techniques. This is particularly useful when studying very small samples (dimensions $\ll$ wavelength). The most common resonant technique used in this frequency range is the so-called cavity perturbation technique, whereby perturbations of the cavity characteristics may be related to the complex electrodynamic response of a sample introduced into the cavity. Such a system has been developed at Montana State University, and at the National High Magnetic Field Laboratory in Tallahassee, for application to a range of problems [1–3]. In particular, this system is ideally suited to EPR investigations in high magnetic fields, as outlined in this paper (see also [3–6]).

2 Experimental Technique

2.1 The Millimeter-Wave Vector Network Analyzer

We use a millimeter-wave vector network analyzer (MVNA [7] manufactured by AB*mm*, 52 Rue Lhomond, 75005 Paris, France) to monitor the phase and amplitude of millimeter-wave radiation transmitted through a resonant cavity containing the sample under investigation. The MVNA allows measurements in a very extended frequency range (continuously sweepable from 8 to ~200 GHz, extendable to ~700 GHz by association with Gunn oscillators) and employs purely solid-state electronics [7].

The principle on which the MVNA operates is as follows: As a nonlinear device, a Schottky diode may be used as a frequency multiplier or harmonic generator (HG), producing frequencies in the millimeter range, $F_{mm} = NF_1$, where F_1 is the source frequency and N is an integer [8]. It is this frequency, F_{mm}, which is then used in an experiment. Similarly, a Schottky diode may be used as a harmonic mixer (HM), down converting the high frequency F_{mm} to a low frequency F_{MHz} (in the MHz range) by mixing it with a similar frequency F_2. If ϕ_1 is the phase noise associated with source S_1, then the phase noise associated with the frequency of interest is $\phi_{mm} = N\phi_1$. The frequency sent from the HM to the vector receiver is then

$$\mathbf{F}_{MHz} = |\mathbf{F}_{mm} - (\mathbf{N}'\times\mathbf{F}_2)| = |\mathbf{N}\times\mathbf{F}_1 - (\mathbf{N}'\times\mathbf{F}_2)| \ , \tag{1}$$

where N' is the harmonic rank at HM. Similarly, the phase noise associated with this frequency will be

$$\boldsymbol{\phi}_{MHz} = |(\mathbf{N}\times\boldsymbol{\phi}_1) - (\mathbf{N}'\times\boldsymbol{\phi}_2)| \ . \tag{2}$$

The basic idea is then to choose the same harmonic $N' = N$ at the source (HG) and at the detector (HM), and to use sources S_1 and S_2 which have identical phase noise $\phi_1 = \phi_2$; the former is achieved by using identical Schottky diodes for HG and HM, while the latter is accomplished by phase locking the sources. In this way, the phase noise cancels, and the frequency F_{MHz} sent to the narrow-band vector receiver (VR) is equal to the frequency difference between the sources S_1 and S_2, multiplied by the harmonic rank, i.e., $F_{MHz} = N|F_1 - F_2|$; the frequencies F_1 and F_2 are programmed so that the detection frequency is 9 MHz. The attraction of this system for spectroscopic purposes is that the amplitude of the signal (frequency F_{MHz}) sent to the VR is proportional to the amplitude of the frequency of interest, F_{mm}, arriving at the HM. In addition, any phase difference ($\delta\phi$) between the frequencies arriving at HM is preserved in the MHz signal, i.e., modification of Eq. (2) gives

$$\boldsymbol{\phi}_{MHz} = \left|\{(\mathbf{N}\times\boldsymbol{\phi}_1) + \boldsymbol{\delta\phi}\} - (\mathbf{N}'\times\boldsymbol{\phi}_2)\right| = \boldsymbol{\delta\phi} \ . \tag{3}$$

Thus, the vector receiver (narrow-band radio) records both the amplitude and the phase of F_{mm} relative to the local oscillator S_2; hence the term "vector" receiver. The phase lock between S_1 and S_2 provides the very low noise floor.

Table 1. Schottky diodes used to cover the frequency range 32–200 GHz.

Band	Harmonic	Frequency range (GHz)	Dynamic range (dB)
Q	3	32–50	110–120
V	4	42–72	110–120
W	5, 6	68–108	100–110
D	6–20	105–200	60–100

The systems at Montana State University and in Tallahassee are based on two Yttrium-Iron-Garnet (YIG) sources (S_1 and S_2) which are continuously tunable in the frequency range 8–18 GHz. Using different pairs of Schottky diodes, it is possible to generate any frequency in the range 8 to ~200 GHz. In practice, the Schottky diodes are optimized to work in certain frequency bands and for certain harmonics; the output power, and therefore the dynamic range of the instrument, is reduced for each successive harmonic, i.e., from N to $N+1$. Table 1 gives details of some of these diodes.

2.2 Experimental Difficulties Associated with High-Field Measurements

The biggest problem associated with performing experiments in high magnetic fields and at low temperatures is that the source and detector (HG and HM) cannot be close to the experiment. In our case, the tail of a ^{4}He cryostat is inserted into the bore of our magnet resulting in a distance in excess of 1.5 m between the magnetic field center and the top of the cryostat. A further complication is that the inner bore diameter of the ^{4}He cryostat is only 20 mm. These dimensions impose severe limitations on the design of any system (probe) for propagating microwave radiation to and from the sample holder.

A schematic of a typical experimental setup is shown in Fig. 1. Rectangular (either Q- or W-band) stainless-steel waveguides are used to propagate polarized mm-wave radiation from the MVNA into the cryostat; for transmission measurements, a second waveguide is necessary to return the transmitted signal to the HM. Stainless steel is used because of its low thermal conductivity. Great care is taken to minimize losses in the probe, e.g., the number of joints are minimized, smooth transitions are inserted wherever changes in the waveguide sizes might lead to impedance mismatches, and all components are highly polished. Because of the fundamental losses associated with the stainless-steel waveguide (~−5 dB/m), the total length used in the probe limits the dynamic range of our instrument. Typical losses in a probe are about −15 dB at 50 GHz, giving an overall dynamic range for the system of between 95 and 105 dB (noise-to-signal ratio of $\ll 1\%$); of course, this figure is unrelated to the ultimate sensitivity of our EPR spectrometer, which depends additionally on factors such as the cavity Q-factor and sample filling factor (see below).

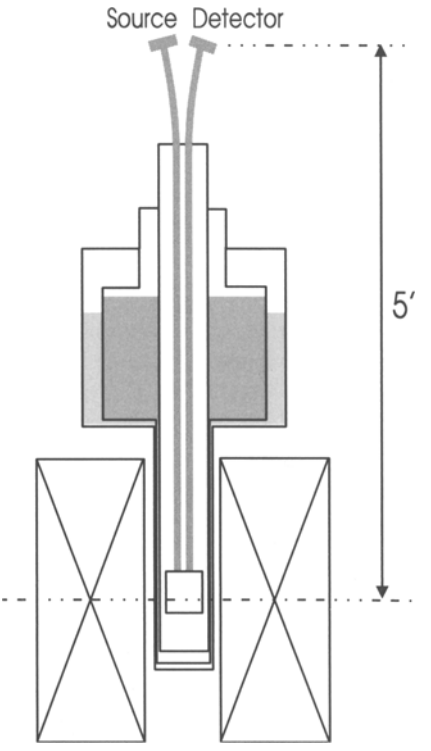

Fig. 1. A schematic of the experimental setup. The magnetic field center is indicated by the dashed line.

A particular advantage of the MVNA is that we can use it as a diagnostic tool when constructing probes for use in high magnetic fields, e.g., we can identify positions in the probe where there may be impedance mismatches or excessive losses.

2.3 Resonant-Cavity-Based Measurements

The use of resonant cavities offers many advantages in this frequency regime, particularly in the case of small crystals, where the radiation wavelength may be quite large compared to the sample dimensions [9, 10]. Due to the highly resonant nature of the problem, the resonance condition is very sensitive to small changes in the sample response to the electromagnetic fields in the cavity. The so-called "cavity perturbation" technique has been used extensively in the past in EPR applications, however, there are few reports which include high magnetic fields. The system described in this work is capable of making measurements in the frequency range $f = \omega/2\pi = 30$ to 120 GHz ($\lambda \sim$ 1–6 mm), and in magnetic fields up to 33 T at the National High Magnetic Field Laboratory.

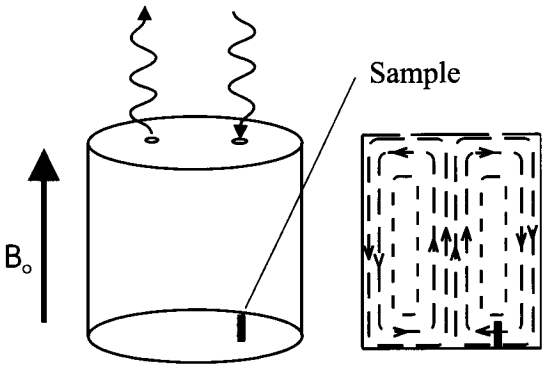

Fig. 2. A schematic of the cavity (3D view to the left) showing the position of the sample at the bottom of the cavity, and (on the right) the AC magnetic field ($\mathbf{B}_1$) distribution within the cavity for the TE011 mode. The DC magnetic field is applied parallel to the cavity axis so that $\mathbf{B}_1$ is perpendicular to $\mathbf{B}_0$ at the sample location.

The strongly enhanced sensitivity of our method is the result of high cavity Q-factors ranging from $5 \cdot 10^3$ to $2 \cdot 10^4$. Thus, our sensitivity is approximately increased by this factor as compared to a conventional single-pass measurement for a sample of comparable size. This enhancement is crucial for the successful measurement of small single crystals.

A range of oversized cylindrical copper (OFHC) cavities are used in transmission, providing several modes in any desired frequency range [1–3]. Predominantly TE01p (p = 1, 2, ...) modes are excited, since these have the highest Q-values and an AC field distribution within the cavity which is highly desirable for EPR measurements. The sample is placed close to the bottom of the cavity, halfway between its axis and its perimeter, thereby ensuring that it is optimally coupled to the radial AC magnetic fields ($\mathbf{B}_1$) for all TE01p modes (this arrangement is shown in Fig. 2). The applied DC magnetic field ($\mathbf{B}_0$) is then directed parallel to the cavity axis so that $\mathbf{B}_1$ is perpendicular to $\mathbf{B}_0$. This configuration enables us to work at a range of different frequencies and fields without the need to interfere with the sample or sample holder.

Using the phase information from the MVNA, we phase lock the source frequency directly to the cavity. A frequency counter can then be used to measure changes in the source frequency and, therefore, the resonance frequency of the cavity, while the cavity Q-factor of the resonance is proportional to the transmitted amplitude [10]. In this mode of operation we can unambiguously discriminate between dissipation and dispersion within the cavity. Dissipation causes changes in the cavity Q-factor, while dispersion results in changes in the resonance frequency. One other advantage of our technique is that it does not require narrow-band magnetic field modulation for detecting resonances. The vector receiver detects at 9 MHz, which is the primary reason for the low noise floor of this system.

2.4 Magnetic Field and Temperature Control

Being constructed from a block of extremely high-conductivity copper, the cavity makes an excellent heat reservoir for controlling the temperature of the sample. Silicone grease is used to keep the sample in good thermal contact with the cavity at all times. A high-resistance wire is used as a heater, by wrapping it several times around the cylindrical cavity. The cavity then sits in low-pressure helium gas which efficiently exchanges heat with a liquid-helium reservoir. Thus, the cavity and the sample can accurately and controllably be maintained at any temperature in the range from 1.25 K up to about 60 K. The temperature is stabilized using a calibrated Cernox resistance thermometer embedded in the walls of the copper cavity; Cernox thermometers have negligible magnetoresistance above 4.2 K. The measurement system is compatible with both superconducting and resistive Bitter-type magnets at Montana State University and at the National High Magnetic Field Laboratory.

3 Representative Results

In order to demonstrate the potential of this technique, we briefly highlight recent results obtained for the Mn_{12} cluster complex $[Mn_{12}O_{12}(CH_3COO)_{16}(H_2O)_4]\cdot 2CH_3COOH\cdot 4H_2O$($Mn_{12}$-Ac) [11]. This system has attracted considerable interest due to indications that it exhibits the phenomenon of magnetic quantum tunneling (MQT) [12]. At low temperatures, the Mn_{12} clusters may be treated as rigid $S = 10$ objects in the presence of a strong uniaxial anisotropy [13]. Recent experiments indicate that these magnetic moments can tunnel through this anisotropy barrier [14]. A purely axially symmetric environment by itself cannot account for the apparent tunneling – a fact which has prompted several authors to argue that one must consider additional effects such as dipolar couplings, hyperfine fields, phonons, and higher-order anisotropy terms [15–17]. The motivation for measuring the EPR response of Mn_{12}-Ac is to attempt to identify, and subsequently quantify, these distortions which must manifest themselves in the EPR spectra. However, the strong axial anisotropy generates substantial zero-field splittings, thus necessitating the need for the high-frequency EPR approach.

The high sensitivity of our technique enables us to study a tiny single crystal – something which has not previously been possible. The typical size of the best available single crystals is $2\times0.2\times0.2$ mm^3, which corresponds to a cavity filling factor of $\sim10^{-4}$. The samples are thus needle-shaped with the needle axis corresponding to the magnetic easy axis. We have performed a range of measurements with the DC magnetic field ($\mathbf{B}_0$) oriented parallel to each of the sample's principal axes [1, 2].

Figure 3 displays a typical set of spectra obtained with the DC magnetic field applied parallel to the sample's easy c-axis. It should be noted that the resonances observed for this orientation correspond to transitions between excited populations, some 40 cm^{-1} (60 k_B) above the ground state. In spite of this, we

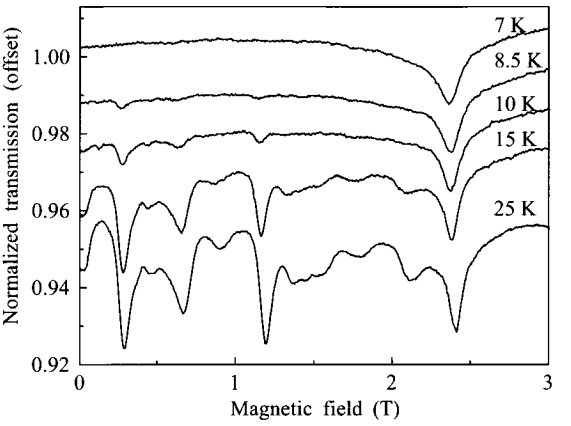

Fig. 3. A set of representative EPR spectra obtained with the DC field oriented parallel to the sample's easy *c*-axis. The frequency is 66 GHz for this measurement.

see transitions down to 10 K, by which time the population of these levels is some three orders of magnitude less than the population of the ground state. By repeating these measurements over a broad frequency range, we can piece together the energy level diagram for this system (this is done in [1, 2, 15]). A compilation of all of the data obtained with the DC field parallel to the *c*-axis is shown in Fig. 4. By extrapolating the data in this figure to zero field, we can deduce five out of the ten zero-field splittings [15, 18]. Furthermore, from the slopes of the straight lines through the data, we are able to directly deduce a *g*-value, i.e., our *g*-value *is not* an adjustable fitting parameter as is the case in other studies of the Mn_{12}-Ac system [16].

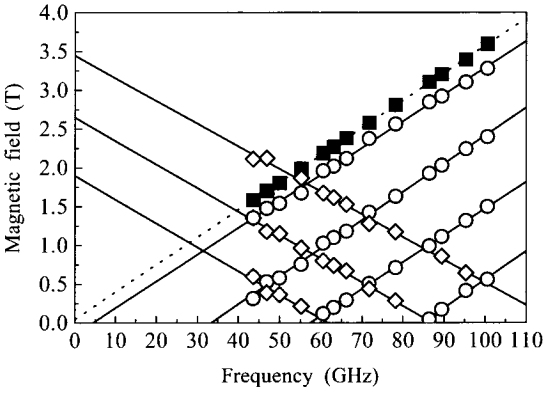

Fig. 4. A compilation of all of the observed resonance fields, plotted against frequency, obtained with the DC field parallel to the *c*-axis. The data may be related to the energy level diagram for the Mn_{12}-Ac system.

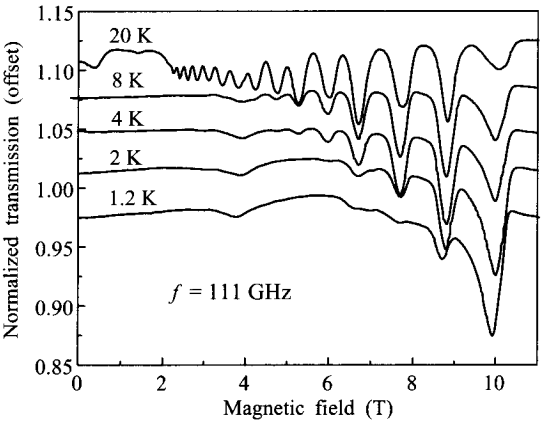

Fig. 5. A set of representative EPR spectra obtained with the DC field oriented perpendicular to the sample's easy c-axis.

Figure 5 shows data obtained with the DC magnetic field oriented perpendicular to the c-axis. For this orientation, transitions involving most of the levels (including the ground state) are accessible, hence the very strong signal even at the lowest temperatures. It should be noted from Figs. 4 and 5, that the data for the two orientations run into each other between 2 and 5 T. By studying a single crystal, we have been able to interpret all of the observed resonances in terms of a recently predicted energy level diagram for the Mn_{12}-Ac system which includes a weak distortion of the axial symmetry (see [4, 5, 15, 18]). This study would not have been possible using powder or polycrystalline samples.

One further point to note: the resonances in Figs. 3 and 5 are rather broad ($\Delta B \sim 0.2$–0.5 T). Extremely large modulation fields (>100 G at 10 kHz) would be required to make a scalar detection of comparable sensitivity. Modulation fields of this magnitude and frequency would not penetrate the cylindrical copper cavities used in this study. Therefore, a comparable sensitivity could only be achieved by an open resonator configuration, e.g., a Fabry-Perot cavity. In addition, one has to be very careful when using field modulation to study systems such as Mn_{12}-Ac, in which the characteristic relaxation processes occur on a time scale comparable to $1/f$, where f is the modulation frequency. Indeed, the dynamics of the relaxation mechanism may be radically altered by field modulation, as shown recently by Perenboom et al. [15].

4 Summary

We have described a multifrequency spectroscopic system which is ideally suited to EPR investigations of very small single crystals. We have demonstrated that this system is capable of providing excellent sensitivity over a broad frequency range and in magnetic fields up to 33 T.

Acknowledgements

This work was supported under PRF no. 33727-G3, NSF-DMR 95-10427 and by the National High Magnetic Field Laboratory (NHMFL).

References

1. Hill S., Sandhu P.S., Buhler C., Uji S., Brooks J.S., Seger L., Boonman M., Wittlin A., Perenboom J.A.A.J., Goy P., Kato R., Sawa H., Aonuma S. in: Millimeter and Submillimeter Waves III (Afsar M.N., ed.), Proc. SPIE, vol. 2842, pp. 296–306 1996.
2. Hill S., Brooks J.S., Qualls J.S., Burgin T., Fravel B., Montgomery L.K., Sarrao J., Fisk Z.: Physica B **246-247**, 110–116 (1998)
3. Boonman M.E.J.: Ph.D. Thesis, University of Nijmegen, Nijmegen, The Netherlands 1998.
4. Hill S., Perenboom J.A.A.J., Dalal N.S., Hathaway T., Stalcup T., Brooks J.S.: Phys. Rev. Lett. **80**, 2453–2456 (1998)
5. Hill S., Perenboom J.A.A.J., Stalcup T., Dalal N.S., Hathaway T., Brooks J.S., Physica B **246-247**, 549–552 (1998)
6. van Dam P.J., Reijerse E.J., Klaassen A.A., Boonman M.E.J., van Bentum P.J.M., Perenboom J. A.A.J., Hagen W.R.: Metal Ions in Biology and Medicine (Collery Ph., Corbella J., Domingo J.L., Etienne J.C., Llobet J.M., eds.), vol. 4, pp. 27–29. Paris: John Libbey Eurotext 1996.
7. Goy P. in: Proc. 15th Int. Conf. in Infrared and Millimeter Waves (Temkin R.J., ed.), Proc. SPIE, vol. 1514, pp. 173–174 1990.
8. LeSurf J.: Millimeter-Wave – Optics, Devices and Systems. London: Adam Hilger 1990.
9. Poole C.P.: Electron Spin Resonance. New York: Interscience 1975.
10. Klein O., Donovan S., Dressel M., Gruner G.: Int. J. Infrared Millimetre Waves **14**, 2423–2457 (1993); Donovan S., Klein O., Dressel M., Gruner G.: ibid. **14**, 2459–2487 (1993); Dressel M., Klein O., Donovan S., Gruner G.: ibid. **14**, 2489–2517 (1993)
11. Lis T.: Acta Cryst. B **36**, 2042–2046 (1980)
12. Gunther L., Barbara B. (eds.): Quantum Tunneling of Magnetization – QTM'94, vol. 301, NATO ASI Series E: Applied Sciences. Dordrecht: Kluwer 1995.
13. Sessoli R., Tsai H-L., Schake A.R., Wang S., Vincent J.B., Folting K., Gatteschi D., Christou G., Hendrickson D.N.: J. Am. Chem. Soc. **115**, 1804–1816 (1993); Caneschi A., Gatteschi D., Sessoli R., Barra A.L., Brunel L.C., Guillot M.: J. Am. Chem. Soc. **113**, 5873–5874 (1991)
14. Friedman J.R., Sarachik M.P., Tejada J., Ziolo R.: Phys. Rev. Lett. **76**, 3830–3834 (1996); Thomas L., Lionti F., Ballou R., Gatteschi D., Sessoli R., Barbara B.: Nature **383**, 145–147 (1996)
15. Perenboom J.A.A.J., Brooks J.S., Hill S., Hathaway T., Dalal N.S.: Phys. Rev. B **58**, 330–338 (1998)
16. Barra A.L., Gatteschi D., Sessoli R.: Phys. Rev. B **56**, 8192–8198 (1997)
17. Politi P., Rettori A., Hartmann-Boutron F., Villain J.: Phys. Rev. Lett. **75**, 537–540 (1995)
18. Perenboom J.A.A.J., Schaapman M.R., Hill S.O., Brooks J.S., Dalal N.S. in: Proc. Physical Phenomena in High Magnetic Fields III (PPHMF-III), (Fisk Z., Dordrecht L., Gor'kov P., Schrieffer J.R., eds.). Tallahassee, Florida, USA, 24–27 October 1998. Singapore: World Scientific 1999.

Authors' address: Dr. Naresh S. Dalal, Department of Chemistry, Florida State University, Tallahassee, FL 32310, USA